Comparison of fast 3D simulation and actinic inspection for EUV masks with buried defects

Chris H. Clifford*[1], Sandy Wiraatmadja[1], Tina T. Chan[2], Andrew R. Neureuther[1], Kenneth A. Goldberg[3], Iacopo Mochi[3], Ted Liang[4]

[1]Department of Electrical Engineering and Computer Sciences, University of California, Berkeley, CA 94720
[2]Department of Bioengineering, University of California, Berkeley, CA 94720
[3] Lawrence Berkeley National Laboratory, 1 Cyclotron Road, Berkeley, CA 94720
[4] Intel Corp., 2200 Mission College blvd., Santa Clara, CA 95054

ABSTRACT

Aerial images for isolated defects and the interactions of defects with features are compared between the Actinic Inspection Tool (AIT) at Lawrence Berkeley National Laboratory (LBNL) and the fast EUV simulation program RADICAL. Comparisons between AIT images from August 2007 and RADICAL simulations are used to extract aberrations. At this time astigmatism was the dominant aberration with a value of 0.55 waves RMS.
Significant improvements in the imaging performance of the AIT were made between August 2007 and December 2008. A good match will be shown between the most recent AIT images and RADICAL simulations without aberrations. These comparisons will demonstrate that a large defect, in this case 7nm tall on the surface, is still printable even if it is centered under the absorber line. These comparisons also suggest that the minimum defect size is between 1.5nm and 0.8nm surface height because a 1.5nm defect was printable but a 0.8nm was not. Finally, the image of a buried defect near an absorber line through focus will demonstrate an inversion in the effect of the defect from a protrusion of the dark line into the space to a protrusion of the space into the line.

Keywords: actinic EUV inspection, fast simulation, buried defect, EUV mask

1. INTRODUCTION

Extreme ultraviolet (EUV) lithography is the leading contender to replace deep ultraviolet lithography for high volume semiconductor manufacturing, but there are still several roadblocks preventing its adoption. A major roadblock currently is the availability of defect free masks along with inspection and review infrastructure [1]. This paper addresses that issue by comparing the results of the fast EUV mask simulator RADICAL [2] with experimental results from the actinic inspection tool (AIT) at Lawrence Berkeley National Lab [3]. These comparisons will help characterize and validate both tools as well as give insight into buried defect printability in EUV lithography.
First, the AIT aberrations present in August 2007 will be extracted by looking at the center intensity and symmetry of a buried defect image through focus. The astigmatism, spherical aberration and coma will be extracted from the through focus image of a single defect. This analysis, however, will end up being unnecessary for comparisons with more recent AIT images, because the quality of the AIT imaging has been dramatically improved from August 2007 to December 2009. The new images will be compared successfully to simulations without aberrations.
These new images will be analyzed to answer the following three questions: Will a covered defect print? What is the maximum allowable defect size? How does the printability of a defect near an absorber feature change through focus?
It is important to note that all of this analysis and simulation was for a nearly coherent illumination, with a sigma of 0.1. So further simulation would be needed to determine how the properties of defects discussed in this paper affect images produced by systems with different illuminations. But, this paper does show that RADICAL, or other accurate near field simulation methods, can accurately predict the complex behavior of a buried EUV defect.

* chris@eecs.berkeley.edu; phone: (651) 238-9628

Alternative Lithographic Technologies, edited by Frank M. Schellenberg, Bruno M. La Fontaine
Proc. of SPIE Vol. 7271, 72711F · © 2009 SPIE · CCC code: 0277-786X/09/$18 · doi: 10.1117/12.813846

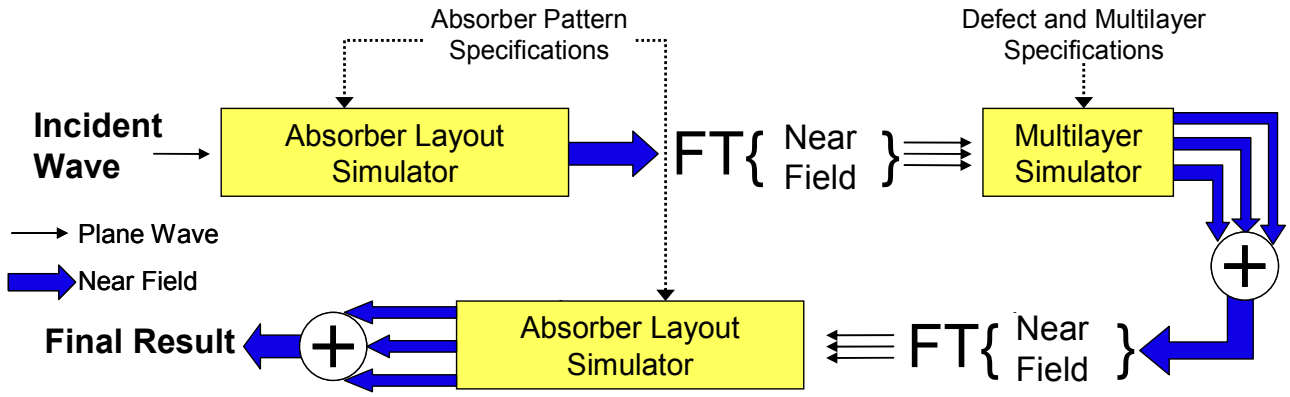

Figure 1. Block Diagram of Radical

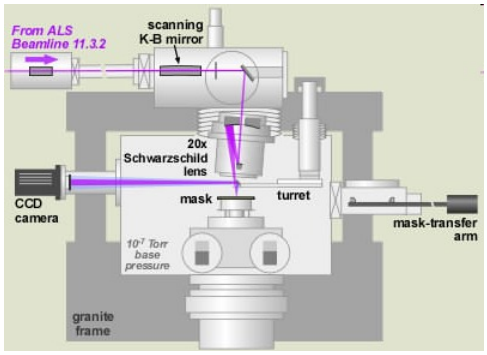

Figure 3. Actinic Inspection Tool (AIT) at Lawrence Berkeley national Lab

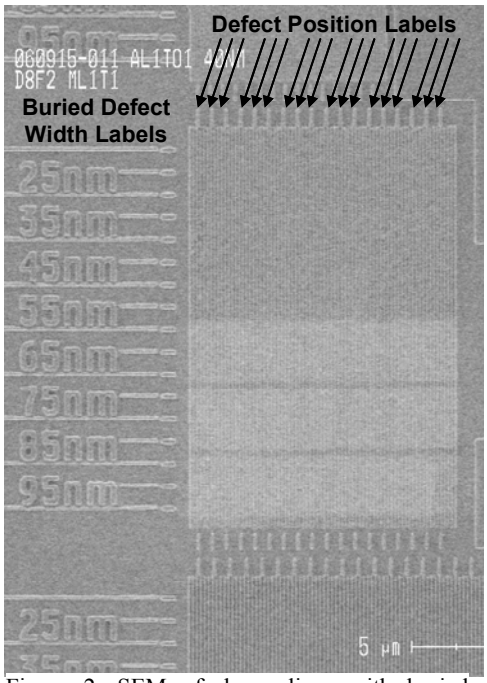

Figure 2. SEM of dense lines with buried defects on programmed defect mask.

2. RADICAL

A new simulator, RADICAL (Rapid Absorber Defect Interaction Computation for Advanced Lithography), was presented in [2] which can simulate EUV masks with buried defects and absorber features two orders of magnitude faster than the finite difference time domain (FDTD) using two orders of magnitude less memory. This speedup is accomplished by simulating the absorber features and defective multilayer separately using simulation methods optimized for each. The simulator flow is shown in Figure 1. The absorber layout simulator runs without regard for the multilayer geometry and the multilayer simulator runs without regard for the absorber layout. This modularity makes the fast and accurate simulation of a large mask area containing buried defects possible.

3. ACTINIC INSPECTION TOOL

The AIT is a direct CCD actinic (EUV-wavelength) EUV mask inspection tool [3]. A shown in Figure 3, it employs a bending magnet at the Advanced Light Source synchrotron at Lawrence Berkeley National Laboratory as its source and uses a Fresnel zone plate lens to project a high-magnification image with numerical aperture values that emulate current EUVL printing tools. Bitmap aerial images recorded by the AIT are suitable for direct comparison with bitmaps from simulation.

Recently the performance of the AIT has been improved greatly, and this is reflected in this paper. The section on aberration extraction uses images recorded on the AIT in August 2007. At this time the AIT had significant aberrations. The section on the effects of buried defects near features, however, used images recorded in December 2008. At this time the AIT aberrations were much lower. Simulations with no aberrations matched these images, as will be shown below. All simulations in this paper will assume a sigma of 0.1 for the AIT. For the isolated defect simulations done in 2007 the NA is 0.25. For the 2008 simulations the NA is 0.3. Also, focus values in this paper represent the mask position.

4. PROGRAMMED DEFECT MASK

All AIT inspections were done on the same programmed defect mask in which 48nm high posts with a square base on a substrate are over-coated with a multilayer. The width of the posts is varied. It turns out that over-coating produced defects which all have between a 50 and 60 nm FWHM diameter and heights ranging up to 8nm [4]. It was shown in [5] that the most critical dimension of an over coated buried defect is

the surface height. Therefore, that will be the only dimension mentioned in this paper. The substrate and surface sizes of all the defects on the mask is given in Table 1. This mask contains areas of isolated defects as well as defects near dense absorber lines. Near the absorber lines the position of the defect relative to the lines is varied allowing the effect of defect location on linewidth change to be studied. An SEM of this area of the mask is shown in Figure 2

Buried Width	Buried Height	Surface Width (FWHM)	Surface Height
100	48	60	8
95	48	59	7
90	48	58	6.2
85	48	56	5.3
80	48	55	4.4
75	48	54	3.5
70	48	53	2.6143
65	48	52	1.7228
60	48	51	0.8313

Table 1. Defect sizes for program defect mask. Buried defects are boxes on the substrate with a square base and constant height. The surface defects are the result of the multilayer smoothing and are roughly Gaussian shaped.

5. ABERRATION EXTRACTION

As stated above, the images taken in August 2007 on the AIT are affected significantly by aberrations. The presence of these aberrations is obvious in the images of isolated buried defects through focus shown in Figure 4. The physical defects in the mask are symmetric, but the AIT images rotate from an ellipse with its major axis pointing northeast at -7.6μm defocus to an ellipse with its major axis pointing northeast for +7.7μm defocus. This is caused by astigmatism, as will be shown below. Before meaningful comparisons between RADICAL and the AIT can be performed, the aberrations of the system need to be known. The magnitude of the aberrations present in the AIT can be extracted by matching the center intensity of through focus AIT images with simulations modeling the aberrations. It turns out that each aberration affects a different feature of the center intensity focus curve, so the extraction does not require the simulation of every possible aberration combination. In fact, each aberration focus combination must only be simulated once, with the other aberrations fixed.

Figure 5 shows the initial comparisons between the center intensity of the buried defect images from RADICAL and the AIT. It is obvious that both the absolute intensities and trends in intensity through focus do not match.

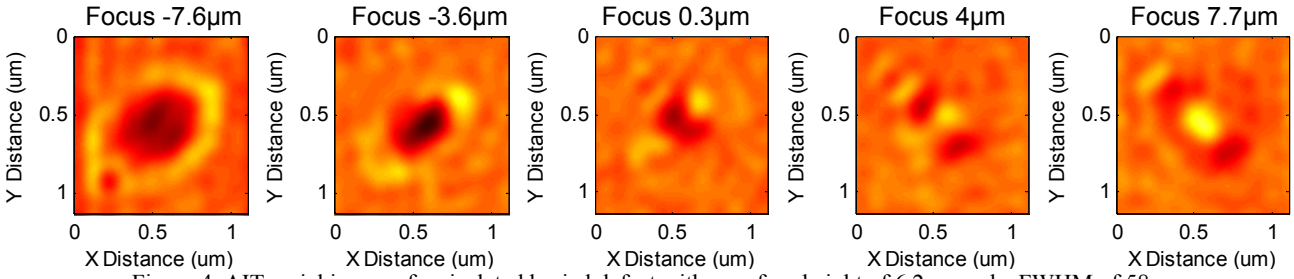

Figure 4. AIT aerial image of an isolated buried defect with a surface height of 6.2nm and a FWHM of 58nm

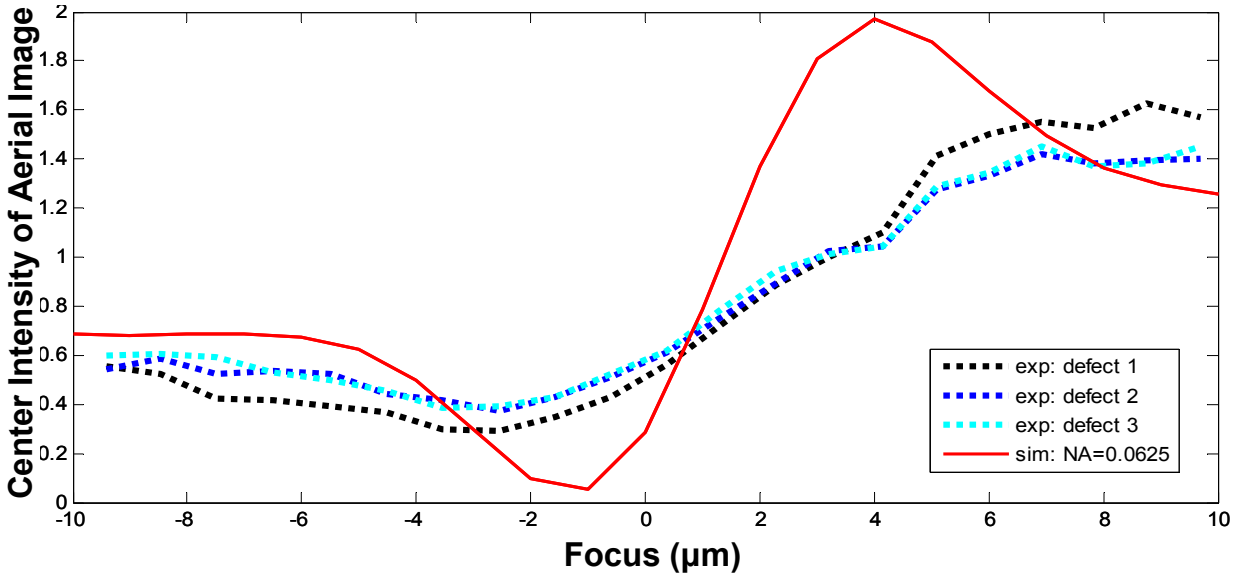

Figure 5. Comparison of center image intensity between RADICAL simulations and experiments. The solid line is the RADICAL simulation with no aberrations included and the dotted lines are the experiment.

Figure 6 shows the simulated aerial image out of focus with increasing levels of astigmatism. The higher the astigmatism the more elliptical and rotated the defect image becomes. This rotation is similar to the rotation in the images in Figure 4. The addition of astigmatism into the simulation also affects the center defect intensity through focus. Figure 8 shows this effect. As astigmatism is increased, the slope of the curve decreases and the maximum and minimum intensity points become less extreme. An astigmatism value of 0.55 matches the slope of the experimental values best around zero defocus.

But, astigmatism is not the only aberration present. As Figure 5 shows, for the high negative defocus region the aerial image center intensity predicted by simulation is higher than the experimental values. This isn't accounted for by the addition of astigmatism. To match this behavior, spherical aberration must be added. Figure 7 shows the effect of adding various levels of spherical aberration to the simulation. There is a minor effect on the slope near zero defocus, a large lateral shift in the curve, and a drop in the center intensity values for the negative defocus region. A spherical aberration level of 0.1 waves RMS matches best in this region.

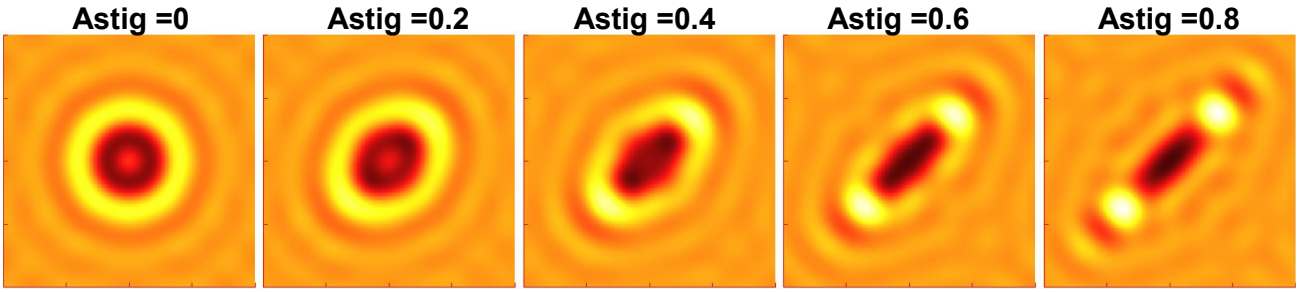

Figure 6. RADICAL simulation of a 6.2nm tall (surface height) buried defect -5µm out of focus with varying astigmatism values. The units on astigmatism are waves RMS.

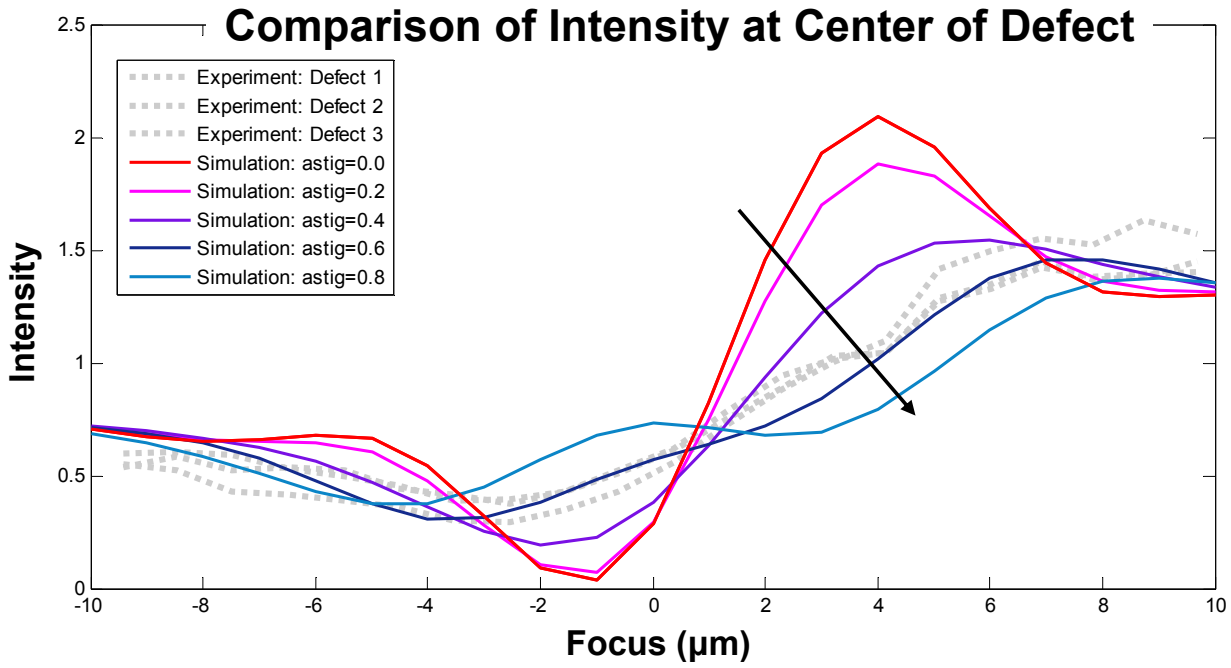

Figure 8. Change is center intensity through focus as a function of astigmatism. The astigmatism tends to flatten the curve.

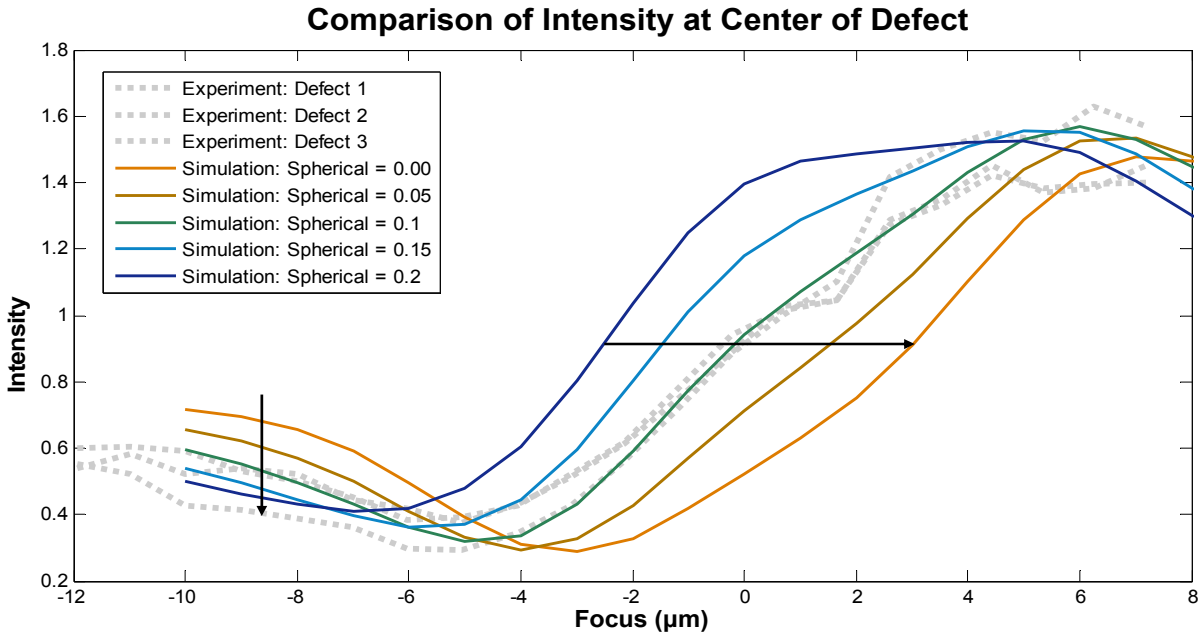

Figure 7. Center intensity through focus as a function of spherical aberration. Spherical changes the best focus position and lowers the center intensity value for very negative defocus values

When these two aberrations are included the center intensity of the simulation matched the AIT experiments very well. But, comparing the images themselves shows one subtle difference. Figure 9 shows the comparison of an AIT image with RADICAL simulation for -4.6µm of defocus. Three coma values are used as examples to show the increasing asymmetry for higher values of coma. A coma value of 0.1 matched the experimental images best.

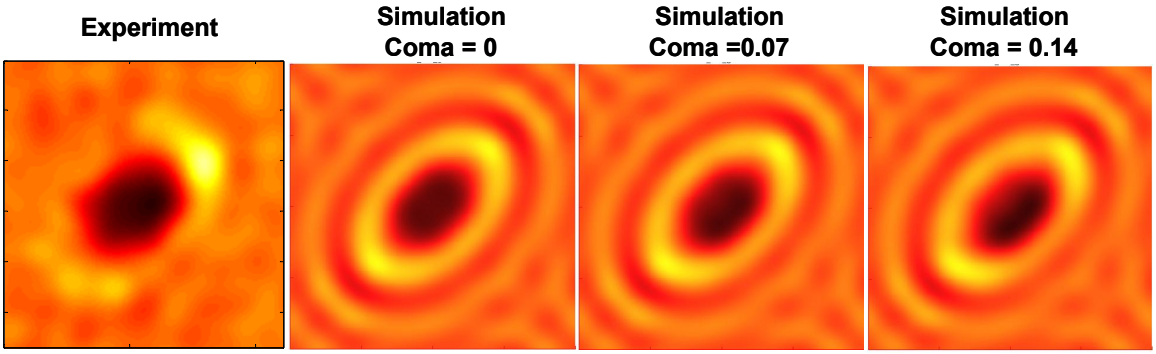

Figure 9. Comparison of experimental aerial image with RADICAL simulation for negative defocus and varying coma values. The asymmetry increases for higher coma values.

The final plot of the center intensity comparison between the AIT images and RADICAL simulations with all included aberrations along with a few example images is shown in Figure 10. These show that the effect of the aberrations on the shapes of the images is predicted correctly by RADICAL, even though the shapes of the images near zero focus were not considered during aberration extraction.

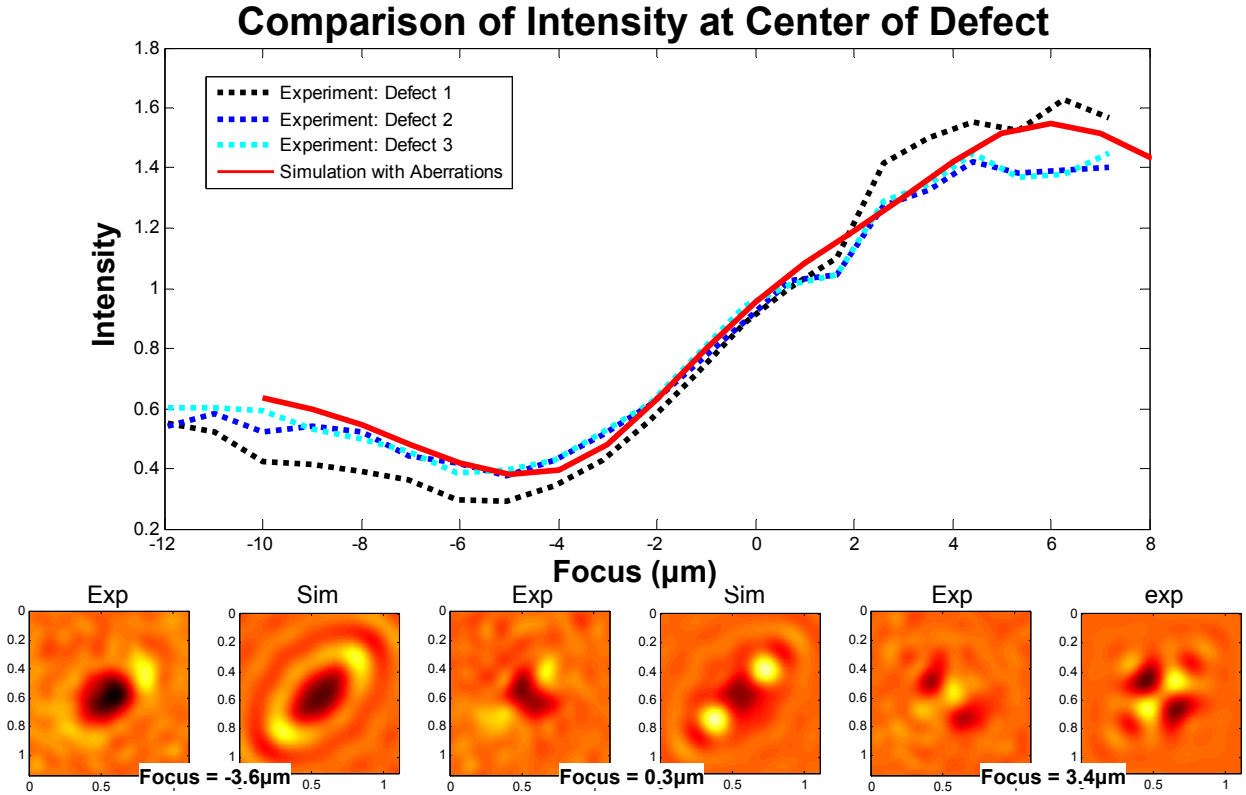

Figure 10. Plot of center intensity of buried defect through focus comparison between RADICAL with astigmatism = 0.55, spherical 0.10 and coma 0.6 waves RMS and experimental AIT images.

6. BURIED DEFECTS NEAR FEATURES

While isolated defects are useful for extracting aberrations and interesting for studying the nature of buried EUV defects, accurately predicting the interaction of buried defects with absorber features is the major need for EUV lithography. The analysis above was for AIT inspections performed in August 2007, which had significant aberrations. It was assumed that the aberrations extracted would be necessary for future comparisons between RADICAL and the AIT. But, it turned out that before the programmed defect mask was inspected again, in December 2009, significant improvements

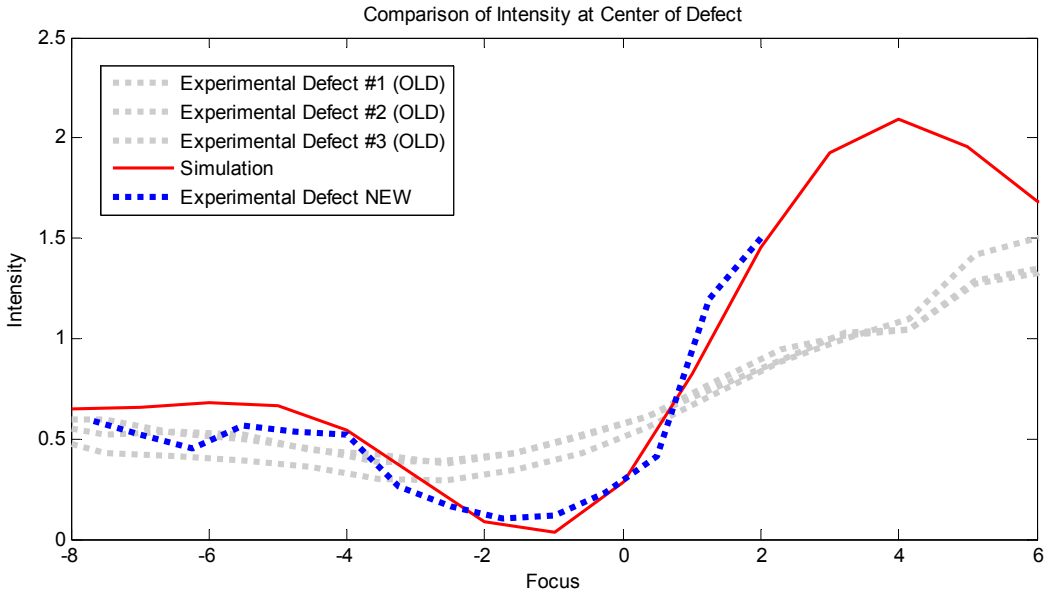

Figure 11. Comparison between the center aerial image intensity predicted by RADICAL simulations and measured on the AIT in December 2008. The three previous curves from 2007 are shown in gray in the background. The 2008 experimental results match the aberration free simulation very well.

had been made to the AIT and the above aberrations were no longer valid. The center defect intensity through focus analysis was repeated and it turned out that an aberration free model was accurate for matching the new data. As Figure 11 shows, the new experimental data matches the aberration free simulations, so the new simulations will be assumed to be aberration free.

There are two goals to this work. The first is to demonstrate the accuracy of the simulation method with comparisons to experiment. The second is to give insight into defect printability. But, it is important to note that while the AIT has an NA similar to a production tool, 0.30, it has a much different illumination. The illumination is nearly coherent, which means the results cannot be transferred directly to production EUV systems.

Three questions will be answered in this study about defect printability in the AIT and then verified with RADICAL simulations. The first question is: will a larger buried defect covered by an absorber line print? As Figure 12 shows, there is a small bump in the AIT image near the defect. The CD drops by as much as 23nm at one point. The results of the simulation show a similar bump, with a 19nm CD change. For 250 lines, these changes are less than 10%. But, for 88nm lines, which would print 22nm wafer lines in a 4x system, 19nm would be an over 20% change.

This shows that a covered defect may print so it is important to fully consider all defects, even if they are covered by absorber features. In this case, the defect is 7nm tall, and 59nm full width half max. But, according to the growth model in [6], which predicts an approximately Gaussian surface profile, the height of the defect at the edge of the absorber pattern is 2.2nm, which corresponds to a round trip path difference for incident light of 0.3λ. This significant fraction of a wavelength should interfere and causes a distortion in the image. This is confirmed by Figure 12.

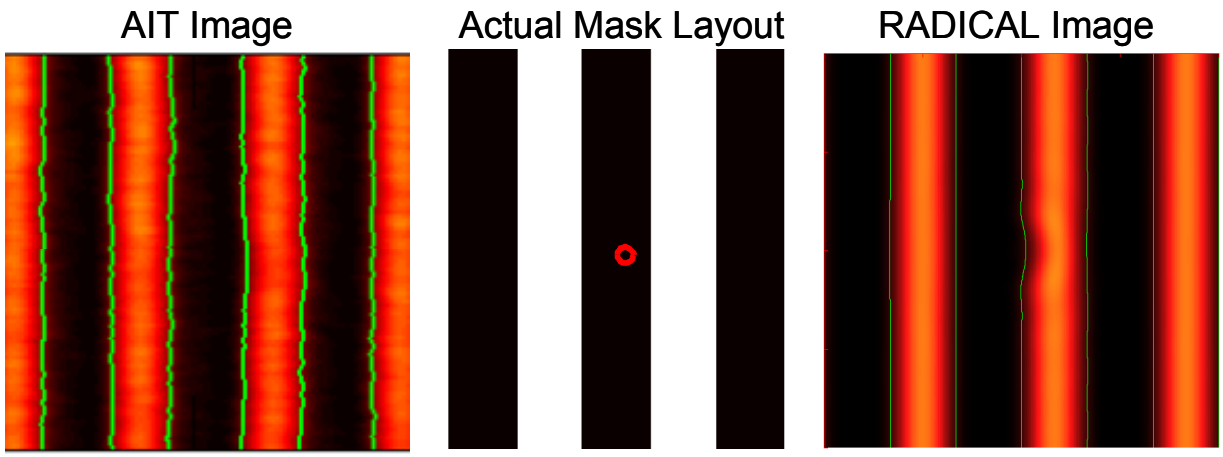

Figure 12. AIT Image, Mask Layout and RADICAL image for covered defect. The defect was 7nm tall and 60nm wide on the multilayer surface. It is centered -43nm from the edge of the lines. The circle in the mask layout represents the position and full width half max of the defect on the surface. The CD change in the AIT image is about 23nm and the CD change in the RADICAL image is 19nm.

The second question is: what is the minimum defect size that will affect printing? The worst case defect position on the programmed defect mask was 57nm from the edge of the line. When looking at AIT images of very small defects, it is difficult to determine what is a result of the defect and what is just roughness on the line. To assist the analysis, the image was visualized as shown in Figure 13. In Figure 13, it is difficult to spot the defects in the aerial image on the left. The CD space map on the right makes it easier. Each column in the figure represents the CD as a function of vertical position in the image on the left. The 1.5nm defect causes an obvious CD change, but the 0.8nm defect does not. So, according to the AIT images, the minimum printable defect is between 1.5nm and 0.8nm surface height. Ideally, the three defects in each image should have the same effect on the CD because they were designed to have the same size and be at the same position. But, they do not. This is most likely an error in the mask. For all of the images of defects in these columns on the mask, for various defect sizes and focus positions, the far left defect was always most printable and the right defect was always least printable. This suggests a variation in alignment, between defect and pattern or a

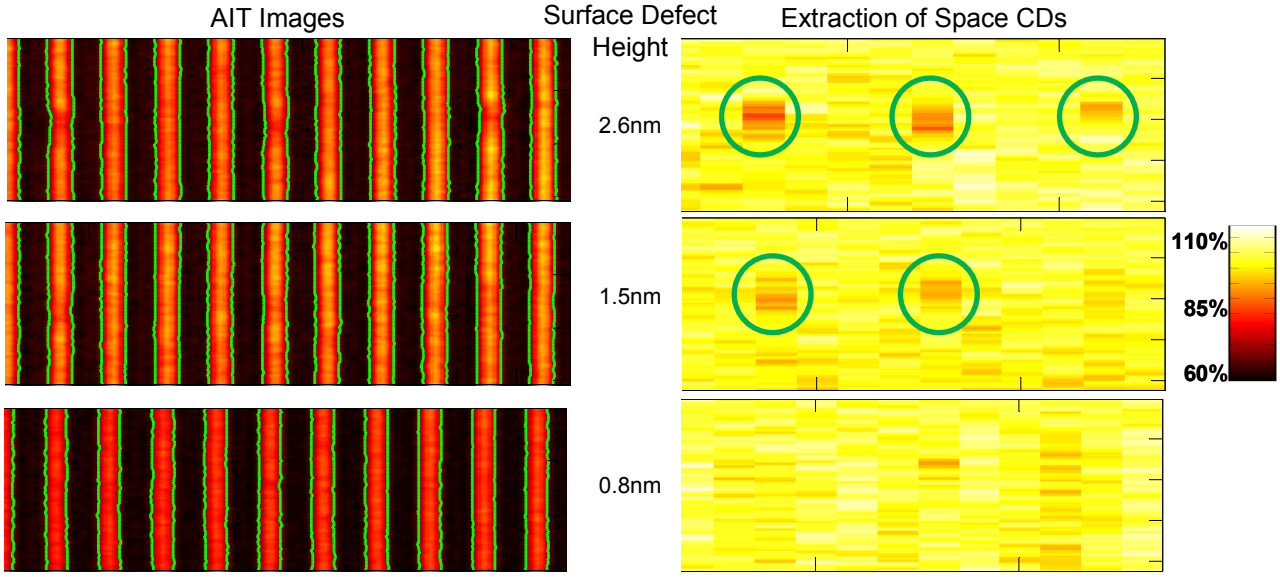

Figure 13. AIT images and map of space CDs for defects centered 57nm form the edge of the line. Each image has three defects. The space CD maps show the space CD as a function of vertical position. The vertical scale is the same as the scale for the images on the left. Each column represents a space (bright area). The circles highlight the effects of the defects. The maximum CD change for the 2.6nm defect was 40nm, the maximum CD change for the 1.5nm defect was 25nm and the there was no change for the 0.8nm defect.

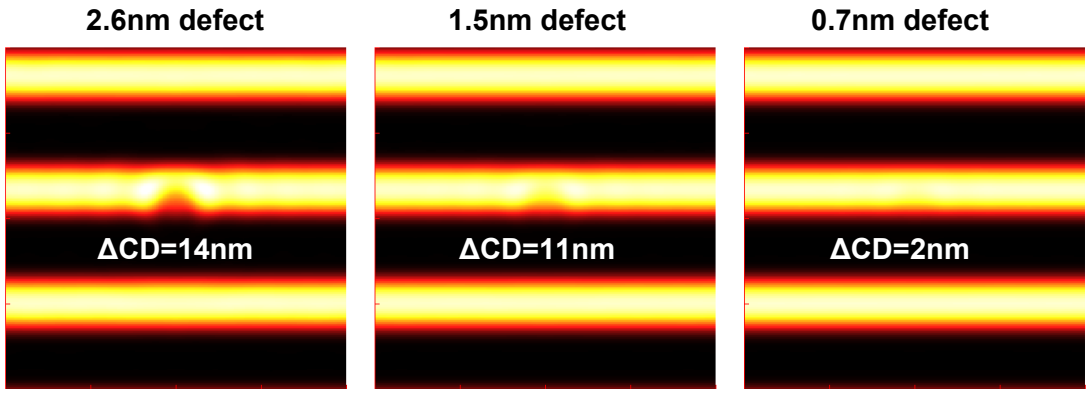

Figure 14. Aerial image predicted by RADICAL simulation of various surface defect heights with the resulting change in CD labeled

variation in defect size in the mask.

The results of the same geometries simulated in RADICAL are shown in Figure 14. The CD changes predicted by RADICAL are lower than what was seen in the AIT. This is most likely because the defect position simulated was not the same as the defect position on the mask. It is also due to the roughness in the lines caused by AIT image noise and actual roughness on the mask. But, RADICAL does confirm that a 1.5nm defect will produce a noticeable CD change and a 0.8nm defect will not.

The final question is: how will a buried defect's printability change through focus. As Figure 11 shows, an isolated defect's center intensity value flips from below the background to above the background through focus. This same effect is observed in buried defects near features, as shown in Figure 15. The top row, the results of RADICAL simulations, shows that for negative defocus, the protrusion of the dark line gets larger, and for positive focus it actually inverts and the bright space protruded into the line. This same behavior is observed in the AIT image. For the focus = 0.5µm case, the effect of the defect is not even visible, but it is for the focus = -1.0µm case. The AIT images match RADICAL very well, demonstrating that RADICAL provides a robust near field model that accurately predicts the effects through focus. It also has implications for defect inspection and process window. An inspection system must be able to inspect through focus, or be sensitive enough to find in focus the very small effect of a buried defect that will have a larger effect out of focus. The fact that defects print worse out of focus may reduce the process window as well.

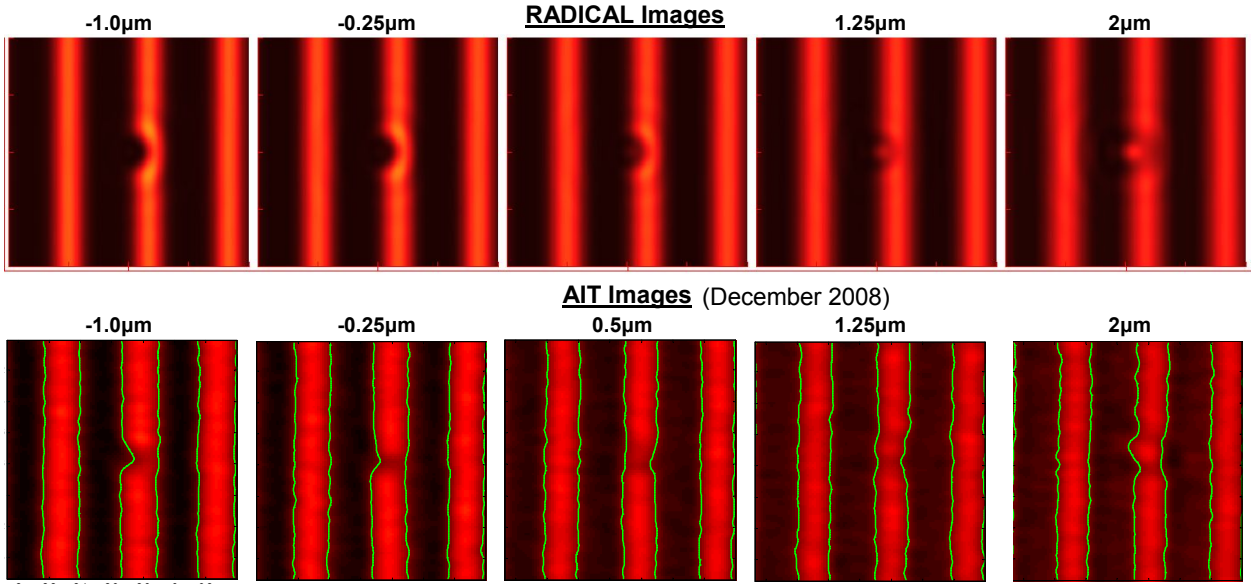

Figure 15. Comparison of aerial images of 5.3nm buried defect on the edge of an absorber line predicted by RADICAL and recorded on the AIT. The label on each image is focus.

7. CONCLUSTION

Comparisons between Aerial images recorded by the Actinic Inspection Tool (AIT) and the fast simulation program RADICAL have demonstrated the quality of AIT images and the accuracy of RADICAL. The AIT aberrations present in August 2007 were extracted by looking at the center intensity and symmetry of a buried defect image through focus. Astigmatism was set by matching the slope of the intensity vs. focus plot, spherical was set matching the defect center intensity for very negative defocus and coma was set by matching the asymmetry of the images.

This analysis, however, proved to be unnecessary for comparisons with more recent AIT images, because the quality of the AIT imaging was dramatically improved from August 2007 to December 2009. The new results, which included images of buried defects near absorber features as well as isolated defects, were analyzed for aberrations in the same way as the previous images and it turned out that they matched aberration free simulations.

Using these new images, it was shown that large defects may print, even if they are covered. The height of the defect in the space near a pattern must be determined. If that height is a non-negligible percentage of the wavelength, then the defect will probably affect printing. AIT images showed that for the worst case position available, 58nm from the edge of the line, a 1.5nm tall defect would print and a 0.8nm defect would not. This trend was confirmed by RADICAL simulations, but the magnitude of the CD changes was difficult to determine because of uncertainties in the experiment.

The effect of a buried defect through focus was demonstrated by the AIT and verified by RADICAL. It was shown that even if a buried defect is hardly noticeable at one focus position it may be very problematic at a different focus position.

It is important to note that all of this analysis and simulation was for nearly coherent illumination with a sigma of 0.1. So further simulation would be needed to determine how the properties of defects discussed in this paper affect images produced by systems with different illuminations. But, this paper does show that the RADICAL, or other accurate near field simulation methods, can accurately predict the complex behavior of a buried EUV defect.

ACKNOWLEDGEMENTS:

This research was funded by a grant from Intel Corp. Aerial image simulations were performed using EMSuite from Panoramic Technology Inc.

[1] Conclusion of Steering Committee at the 2008 EUVL Symposium
[2] Clifford, C. H., et al. “Fast Three-Dimensional Simulation of Buried EUV Mask Defect Interaction with Absorber Features,” Proc. of SPIE 6730, (2007).
[3] K. A. Goldberg, et al. “Performance of actinic EUVL mask imaging using a zoneplate microscope,” Proc. SPIE Photomask (BACUS) 6730, (2007)
[4] T. Liang, et al, “Growth and printability of multilayer phase defects on extreme ultraviolet mask blanks,” J. Vac. Sci. Technol., B25(6), 2098 (2007)
[5] Clifford, C. H., et al. “Smoothing based fast model for images of isolated buried EUV multilayer defects,” Proc. of SPIE 6921, (2008).
[6] Stearns, D.G., et al., “Localized defects in multilayer coatings”, Thin Solid Films 446 Issue 1, 37-49 (2004).